

# PointNet: Deep Learning on Point Sets for 3D Classification and Segmentation

Charles R. Qi\*   Hao Su\*   Kaichun Mo   Leonidas J. Guibas  
 Stanford University

## Abstract

Point cloud is an important type of geometric data structure. Due to its irregular format, most researchers transform such data to regular 3D voxel grids or collections of images. This, however, renders data unnecessarily voluminous and causes issues. In this paper, we design a novel type of neural network that directly consumes point clouds, which well respects the permutation invariance of points in the input. Our network, named **PointNet**, provides a unified architecture for applications ranging from object classification, part segmentation, to scene semantic parsing. Though simple, PointNet is highly efficient and effective. Empirically, it shows strong performance on par or even better than state of the art. Theoretically, we provide analysis towards understanding of what the network has learnt and why the network is robust with respect to input perturbation and corruption.

## 1. Introduction

In this paper we explore deep learning architectures capable of reasoning about 3D geometric data such as point clouds or meshes. Typical convolutional architectures require highly regular input data formats, like those of image grids or 3D voxels, in order to perform weight sharing and other kernel optimizations. Since point clouds or meshes are not in a regular format, most researchers typically transform such data to regular 3D voxel grids or collections of images (e.g. views) before feeding them to a deep net architecture. This data representation transformation, however, renders the resulting data unnecessarily voluminous — while also introducing quantization artifacts that can obscure natural invariances of the data.

For this reason we focus on a different input representation for 3D geometry using simply point clouds — and name our resulting deep nets *PointNets*. Point clouds are simple and unified structures that avoid the combinatorial irregularities and complexities of meshes, and thus are easier to learn from. The PointNet, however,

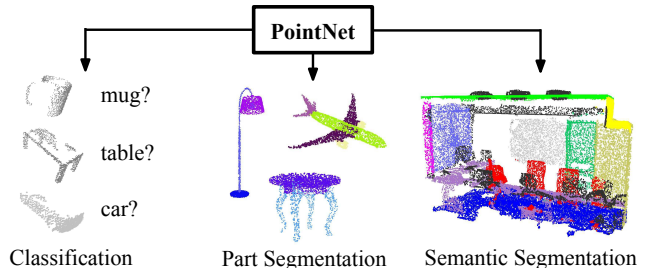


Figure 1. **Applications of PointNet.** We propose a novel deep net architecture that consumes raw point cloud (set of points) without voxelization or rendering. It is a unified architecture that learns both global and local point features, providing a simple, efficient and effective approach for a number of 3D recognition tasks.

still has to respect the fact that a point cloud is just a set of points and therefore invariant to permutations of its members, necessitating certain symmetrizations in the net computation. Further invariances to rigid motions also need to be considered.

Our PointNet is a unified architecture that directly takes point clouds as input and outputs either class labels for the entire input or per point segment/part labels for each point of the input. The basic architecture of our network is surprisingly simple as in the initial stages each point is processed identically and independently. In the basic setting each point is represented by just its three coordinates  $(x, y, z)$ . Additional dimensions may be added by computing normals and other local or global features.

Key to our approach is the use of a single symmetric function, max pooling. Effectively the network learns a set of optimization functions/criteria that select interesting or informative points of the point cloud and encode the reason for their selection. The final fully connected layers of the network aggregate these learnt optimal values into the global descriptor for the entire shape as mentioned above (shape classification) or are used to predict per point labels (shape segmentation).

Our input format is easy to apply rigid or affine transformations to, as each point transforms independently. Thus we can add a data-dependent spatial transformer network that attempts to canonicalize the data before the PointNet processes them, so as to further improve the results.

\* indicates equal contributions.

We provide both a theoretical analysis and an experimental evaluation of our approach. We show that our network can approximate any set function that is continuous. More interestingly, it turns out that our network learns to summarize an input point cloud by a sparse set of key points, which roughly corresponds to the skeleton of objects according to visualization. The theoretical analysis provides an understanding why our PointNet is highly robust to small perturbation of input points as well as to corruption through point insertion (outliers) or deletion (missing data).

On a number of benchmark datasets ranging from shape classification, part segmentation to scene segmentation, we experimentally compare our PointNet with state-of-the-art approaches based upon multi-view and volumetric representations. Under a unified architecture, not only is our PointNet much faster in speed, but it also exhibits strong performance on par or even better than state of the art.

The key contributions of our work are as follows:

- We design a novel deep net architecture suitable for consuming unordered point sets in 3D;
- We show how such a net can be trained to perform 3D shape classification, shape part segmentation and scene semantic parsing tasks;
- We provide thorough empirical and theoretical analysis on the stability and efficiency of our method;
- We illustrate the 3D features computed by the selected neurons in the net and develop intuitive explanations for its performance.

The problem of processing unordered sets by neural nets is a very general and fundamental problem – we expect that our ideas can be transferred to other domains as well.

## 2. Related Work

**Point Cloud Features** Most existing features for point cloud are handcrafted towards specific tasks. Point features often encode certain statistical properties of points and are designed to be invariant to certain transformations, which are typically classified as intrinsic [2, 21, 3] or extrinsic [18, 17, 13, 10, 5]. They can also be categorized as local features and global features. For a specific task, it is not trivial to find the optimal feature combination.

**Deep Learning on 3D Data** 3D data has multiple popular representations, leading to various approaches for learning. **Volumetric CNNs**: [25, 15, 16] are the pioneers applying 3D convolutional neural networks on voxelized shapes. However, volumetric representation is constrained by its resolution due to data sparsity and computation cost of 3D convolution. FPN [12] and Vote3D [23] proposed special methods to deal with the sparsity problem; however,

their operations are still on sparse volumes, it's challenging for them to process very large point clouds. **Multiview CNNs**: [20, 16] have tried to render 3D point cloud or shapes into 2D images and then apply 2D conv nets to classify them. With well engineered image CNNs, this line of methods have achieved dominating performance on shape classification and retrieval tasks [19]. However, it's nontrivial to extend them to scene understanding or other 3D tasks such as point classification and shape completion. **Spectral CNNs**: Some latest works [4, 14] use spectral CNNs on meshes. However, these methods are currently constrained on manifold meshes such as **organic** objects and it's not obvious how to extend them to non-isometric shapes such as furniture. **Feature-based DNNs**: [6, 8] firstly convert the 3D data into a vector, by extracting traditional shape features and then use a fully connected net to classify the shape. We think they are constrained by the representation power of the features extracted.

**Deep Learning on Unordered Sets** From a data structure point of view, a point cloud is an unordered set of vectors. While most works in deep learning focus on regular input representations like sequences (in speech and language processing), images and volumes (video or 3D data), not much work has been done in deep learning on point sets.

One recent work from Oriol Vinyals et al [22] looks into this problem. They use a read-process-write network with attention mechanism to consume unordered input sets and show that their network has the ability to sort numbers. However, since their work focuses on generic sets and NLP applications, there lacks the role of geometry in the sets.

## 3. Problem Statement

We design a deep learning framework that directly consumes unordered point sets as inputs. A point cloud is represented as a set of 3D points  $\{P_i | i = 1, \dots, n\}$ , where each point  $P_i$  is a vector of its  $(x, y, z)$  coordinate plus extra feature channels such as color, normal etc. For simplicity and clarity, unless otherwise noted, we only use the  $(x, y, z)$  coordinate as our point's channels.

For the object classification task, the input point cloud is either directly sampled from a shape or pre-segmented from a scene point cloud. Our proposed deep network outputs  $k$  scores for all the  $k$  candidate classes. For semantic segmentation, the input can be a single object for part region segmentation, or a sub-volume from a 3D scene for object region segmentation. Our model will output  $n \times m$  scores for each of the  $n$  points and each of the  $m$  semantic sub-categories.

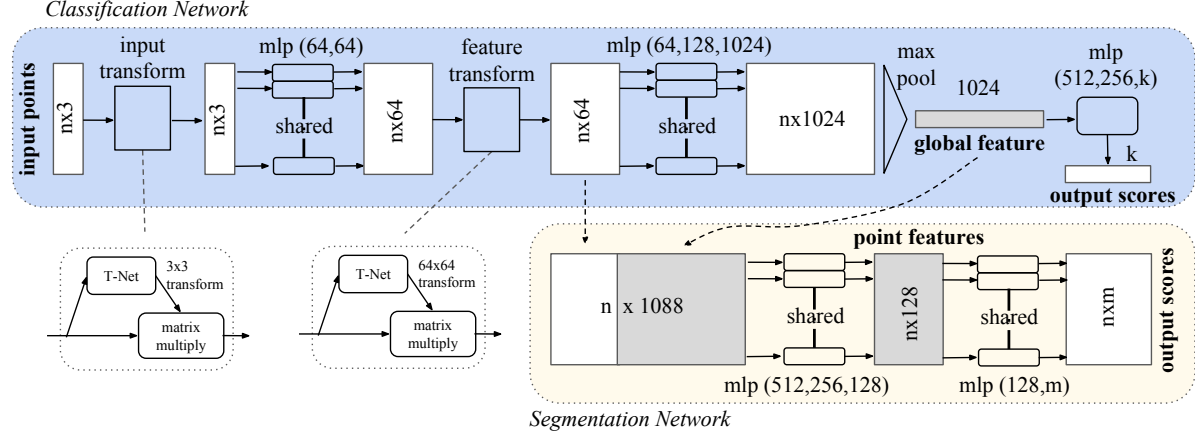


Figure 2. **PointNet Architecture.** The classification network takes  $n$  points as input, applies input and feature transformations, and then aggregates point features by max pooling. The output is classification scores for  $k$  classes. The segmentation network is an extension to the classification net. It concatenates global and local features and outputs per point scores. “mlp” stands for multi-layer perceptron, numbers in bracket are layer sizes. Batchnorm is used for all layers with ReLU. Dropout layers are used for the last mlp in classification net.

## 4. Deep Learning on Point Sets

The architecture of our network (Sec 4.2) is inspired by the properties of point sets in  $\mathbb{R}^n$  (Sec 4.1).

### 4.1. Properties of Point Sets in $\mathbb{R}^n$

Our input is a subset of points from an Euclidean space. It has three main properties:

- **Unordered.** Unlike pixel arrays in images or voxel arrays in volumetric grids, point cloud is a set of points without specific order. In other words, a network that consumes  $N$  3D point sets needs to be invariant to  $N!$  permutations of the input set in data feeding order.
- **Interaction among points.** The points are from a space with a distance metric. It means that points are not isolated, and neighboring points form a meaningful subset. Therefore, the model needs to be able to capture local structures from nearby points, and the combinatorial interactions among local structures.
- **Invariance under transformations.** As a geometric object, the learned representation of the point set should be invariant to certain transformations. For example, rotating and translating points all together should not modify the global point cloud category nor the segmentation of the points.

### 4.2. PointNet Architecture

Our full network architecture is visualized in Fig 2, where the classification network and the segmentation network share a great portion of structures. Please read the caption of Fig 2 for the pipeline.

Our network has three key modules: the max pooling layer as a symmetric function to aggregate information from

all the points, a local and global information combination structure, and two joint alignment networks that align both input points and point features.

We will discuss our reason behind these design choices in separate paragraphs below.

**Symmetry Function for Unordered Input** In order to make a model invariant to input permutation, three strategies exist: 1) sort input into a canonical order; 2) treat the input as a sequence to train an RNN, but augment the training data by all kinds of permutations; 3) use a simple symmetric function to aggregate the information from each point. Here, a symmetric function takes  $n$  vectors as input and outputs a new vector that is invariant to the input order. For example,  $+$  and  $*$  operators are symmetric binary functions.

While sorting sounds like a simple solution, in high dimensional space there in fact does not exist an ordering that is stable w.r.t. point perturbations in the general sense. This can be easily shown by contradiction. If such an ordering strategy exists, it defines a bijection map between a high-dimensional space and a 1d real line. It is not hard to see, to require an ordering to be stable w.r.t point perturbations is equivalent to requiring that this map preserves spatial proximity as the dimension reduces, a task that cannot be achieved in the general case. Therefore, sorting does not fully resolve the ordering issue, and it’s hard for a network to learn a consistent mapping from input to output as the ordering issue persists. As shown in experiments (Fig 5), we find that applying a MLP directly on the sorted point set performs poorly, though slightly better than directly processing an unsorted input.

The idea to use RNN considers the point set as a sequential signal and hopes that by training the RNN

with randomly permuted sequences, the RNN will become invariant to input order. However in “OrderMatters” [22] the authors have shown that order does matter and cannot be totally omitted. While RNN has relatively good robustness to input ordering for sequences with small length (dozens), it’s hard to scale to thousands of input elements, which is the common size for point sets. Empirically, we have also shown that model based on RNN does not perform as well as our proposed method (Fig 5).

Our idea is to approximate a general function defined on a point set by applying a symmetric function on transformed elements in the set:

$$f(\{x_1, \dots, x_n\}) \approx g(h(x_1), \dots, h(x_n)), \quad (1)$$

where  $f : 2^{\mathbb{R}^N} \rightarrow \mathbb{R}$ ,  $h : \mathbb{R}^N \rightarrow \mathbb{R}^K$  and  $g : \underbrace{\mathbb{R}^K \times \dots \times \mathbb{R}^K}_n \rightarrow \mathbb{R}$  is a symmetric function.

Empirically, our basic module is very simple: we approximate  $h$  by a multi-layer perceptron network and  $g$  by a composition of a single variable function and a max pooling function. This is found to work well by experiments. Through a collection of  $h$ , we can learn a number of  $f$ ’s to capture different properties of the set.

While our key module seems simple, it has interesting properties (see Sec 5.3) and can achieve strong performance (see Sec 5.1) in a few different applications. Due to the simplicity of our module, we are also able to provide theoretical analysis as in Sec 4.3.

**Local and Global Information Aggregation** The output from the above section forms a vector  $[f_1, \dots, f_K]$ , which is a global signature of the input set. We can easily train a SVM or multi-layer perceptron classifier on the shape global features for classification. However, point segmentation requires a combination of local and global knowledge. We can achieve this by a simple yet highly effective manner.

Our solution can be seen in Fig 2 (*Segmentation Network*). After computing the global point cloud feature vector, we feed it back to per point features by concatenating the global feature with each of the point features. Then we extract new per point features based on the combined point features - this time the per point feature is aware of both the local and global information.

With this modification our network is able to predict per point quantities that rely on both local geometry and global semantics. For example we can accurately predict per-point normals (fig in supplementary), validating that the network is able to summarize information from the point’s local neighborhood. In experiment session, we also show that our model can achieve state-of-the-art performance on shape part segmentation and scene segmentation.

**Joint Alignment Network** The semantic labeling of a point cloud has to be invariant if the point cloud undergoes certain geometric transformations, such as rigid transformation. We therefore expect that the learnt representation by our point set is invariant to these transformations.

A natural solution is to align all input set to a canonical space before feature extraction. Jaderberg et al. [9] introduces the idea of spatial transformer to align 2D images through sampling and interpolation, achieved by a specifically tailored layer implemented on GPU.

Our input form of point clouds allows us to achieve this goal in a much simpler way compared with [9]. We do not need to invent any new layers and no alias is introduced as in the image case. We predict an affine transformation matrix by a mini-network (T-net in Fig 2) and directly apply this transformation to the coordinates of input points. The mini-network itself resembles the big network and is composed by basic modules of point independent feature extraction, max pooling and fully connected layers. More details about the T-net are in the supplementary.

This idea can be further extended to the alignment of feature space, as well. We can insert another alignment network on point features and predict a feature transformation matrix to align features from different input point clouds. However, transformation matrix in the feature space has much higher dimension than the spatial transform matrix, which greatly increases the difficulty of optimization. We therefore add a regularization term to our softmax training loss. We constrain the feature transformation matrix to be close to orthogonal matrix:

$$L_{reg} = \|I - AA^T\|_F^2, \quad (2)$$

where  $A$  is the feature alignment matrix predicted by a mini-network. An orthogonal transformation will not lose information in the input, thus is desired. We find that by adding the regularization term, the optimization becomes more stable and our model achieves better performance.

### 4.3. Theoretical Analysis

**Universal approximation** We first show the universal approximation ability of our neural network to continuous set functions. By the continuity of set functions, intuitively, a small perturbation to the input point set should not greatly change the function values, such as classification or segmentation scores.

Formally, let  $\mathcal{X} = \{S : S \subseteq [0, 1]^m \text{ and } |S| = n\}$ ,  $f : \mathcal{X} \rightarrow \mathbb{R}$  is a continuous set function on  $\mathcal{X}$  w.r.t to Hausdorff distance  $d_H(\cdot, \cdot)$ , i.e.,  $\forall \epsilon > 0, \exists \delta > 0$ , for any  $S, S' \in \mathcal{X}$ , if  $d_H(S, S') < \delta$ , then  $|f(S) - f(S')| < \epsilon$ . Our theorem says that  $f$  can be arbitrarily approximated by our network given enough neurons at the max pooling layer, i.e.,  $K$  in (1) is sufficiently large.



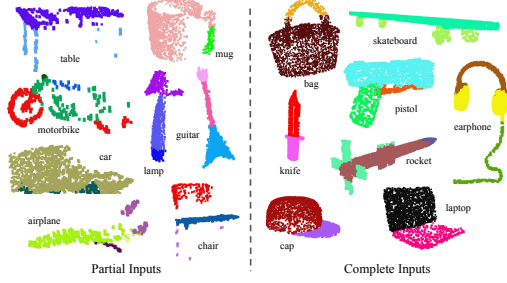


Figure 3. **Qualitative results for part segmentation.** We visualize the CAD part segmentation results across all 16 object categories. We show both results for partial simulated Kinect scans (left block) and complete ShapeNet CAD models (right block).

**Theorem 1** Suppose  $f : \mathcal{X} \rightarrow \mathbb{R}$  is a continuous set function w.r.t Hausdorff distance  $d_H(\cdot, \cdot)$ .  $\forall \epsilon > 0, \exists$  a continuous function  $h$  and a symmetric function  $g(x_1, \dots, x_n) = \gamma \circ \text{MAX}$ , such that for any  $S \in \mathcal{X}$ ,

$$\left| f(S) - \gamma \left( \text{MAX}_{x_i \in S} \{h(x_i)\} \right) \right| < \epsilon$$

where  $x_1, \dots, x_n$  is the full list of elements in  $S$  ordered arbitrarily,  $\gamma$  is a continuous function, and  $\text{MAX}$  is a vector max operator that takes  $n$  vectors as input and returns a new vector of the element-wise maximum.

The proof to this theorem can be found in our supplementary material. The key idea is that in the worst case the network can learn to convert a point cloud into a volumetric representation, by partitioning the space into equal-sized voxels. In practice, however, the network learns a much smarter strategy to probe the space, as we shall see in point function visualizations.

**Bottleneck dimension and stability** Theoretically and experimentally we find that the expressiveness of our network is strongly affected by the dimension of the max pooling layer, i.e.,  $K$  in (1). Here we provide an analysis, which also reveals properties related to the stability of our model.

We define  $\mathbf{u} = \text{MAX}_{x_i \in S} \{h(x_i)\}$  to be the sub-network of  $f$  which maps a point set in  $[0, 1]^m$  to a  $K$ -dimensional vector. The following theorem tells us that small corruptions or extra noise points in the input set are not likely to change the output of our network:

**Theorem 2** Suppose  $\mathbf{u} : \mathcal{X} \rightarrow \mathbb{R}^K$  such that  $\mathbf{u} = \text{MAX}_{x_i \in S} \{h(x_i)\}$  and  $f = \gamma \circ \mathbf{u}$ . Then,

(a)  $\forall S, \exists \mathcal{C}_S, \mathcal{N}_S \subseteq \mathcal{X}, f(T) = f(S)$  if  $\mathcal{C}_S \subseteq T \subseteq \mathcal{N}_S$ ;

(b)  $|\mathcal{C}_S| \leq K$

	input	#views	accuracy avg. class	accuracy overall
SPH [11]	mesh	-	68.2	-
3DShapeNets [25]	volume	1	77.3	84.7
VoxNet [15]	volume	12	83.0	85.9
Subvolume [16]	volume	20	86.0	<b>89.2</b>
LFD [25]	image	10	75.5	-
MVCNN [20]	image	80	<b>90.1</b>	-
Ours baseline	point	-	72.6	77.4
Ours PointNet	point	1	86.2	<b>89.2</b>

Table 1. **Classification results on ModelNet40.** Our net achieves state-of-the-art among deep nets on 3D input.

We explain the implications of the theorem. (a) says that  $f(S)$  is unchanged up to the input corruption if all points in  $\mathcal{C}_S$  are preserved; it is also unchanged with extra noise points up to  $\mathcal{N}_S$ . (b) says that  $\mathcal{C}_S$  only contains a bounded number of points, determined by  $K$  in (1). In other words,  $f(S)$  is in fact totally determined by a finite subset  $\mathcal{C}_S \subseteq S$  of less or equal to  $K$  elements. We therefore call  $\mathcal{C}_S$  the **critical point set** of  $S$  and  $K$  the **bottleneck dimension** of  $f$ .

Combined with the continuity of  $h$ , this explains the robustness of our model w.r.t point perturbation, corruption and extra noise points. The robustness is gained in analogy to the sparsity principle in machine learning models. **Intuitively, our network learns to summarize a shape by a sparse set of key points.** In experiment section we see that the key points form the skeleton of an object.

## 5. Experiment

Experiments are divided into four parts. First, we show PointNets can be applied to multiple 3D recognition tasks (Sec 5.1). Second, we provide detailed experiments to validate our network design (Sec 5.2). At last we visualize what the network learns (Sec 5.3) and analyze time and space complexity (Sec 5.4).

### 5.1. Applications

In this section we show how our network can be trained to perform 3D object classification, object part segmentation and semantic scene segmentation<sup>1</sup>. Even though we are working on a brand new data representation (point sets), we are able to achieve comparable or even better performance on benchmarks for several tasks.

**3D Object Classification** Our network learns global point cloud feature that can be used for object classification. We evaluate our model on the **ModelNet40 [25] shape classification benchmark**. There are 12,311 CAD models from 40 man-made object categories, split into 9,843 for

<sup>1</sup>More application examples such as correspondence and point cloud based CAD model retrieval are included in supplementary material.

	mean	aero	bag	cap	car	chair	ear phone	guitar	knife	lamp	laptop	motor	mug	pistol	rocket	skate board	table
# shapes		2690	76	55	898	3758	69	787	392	1547	451	202	184	283	66	152	5271
Wu [24]	-	63.2	-	-	-	73.5	-	-	-	74.4	-	-	-	-	-	-	74.8
Yi [26]	81.4	81.0	78.4	77.7	<b>75.7</b>	87.6	61.9	<b>92.0</b>	85.4	<b>82.5</b>	<b>95.7</b>	<b>70.6</b>	91.9	<b>85.9</b>	53.1	69.8	75.3
3DCNN	79.4	75.1	72.8	73.3	70.0	87.2	63.5	88.4	79.6	74.4	93.9	58.7	91.8	76.4	51.2	65.3	77.1
Ours	<b>83.7</b>	<b>83.4</b>	<b>78.7</b>	<b>82.5</b>	74.9	<b>89.6</b>	<b>73.0</b>	91.5	<b>85.9</b>	80.8	95.3	65.2	<b>93.0</b>	81.2	<b>57.9</b>	<b>72.8</b>	<b>80.6</b>

Table 2. **Segmentation results on ShapeNet part dataset.** Metric is mIoU(%) on points. We compare with two traditional methods [24] and [26] and a 3D fully convolutional network baseline proposed by us. Our PointNet method achieved the state-of-the-art in mIoU.

training and 2,468 for testing. While previous methods focus on volumetric and multi-view image representations, we are the first to directly work on raw point cloud.

We uniformly sample 1024 points on mesh faces according to face area and normalize them into a unit sphere. During training we augment the point cloud on-the-fly by randomly rotating the object along the up-axis and jitter the position of each points by a Gaussian noise with zero mean and 0.02 standard deviation.

In Table 1, we compare our model with previous works as well as our baseline using MLP on traditional features extracted from point cloud (point density, D2, shape contour etc.). Our model achieved state-of-the-art performance among methods based on 3D input (volumetric and point cloud). With only fully connected layers and max pooling, our net gains a strong lead in inference speed and can be easily parallelized in CPU as well. There is still a small gap between our method and multi-view based method (MVCNN [20]), which we think is due to the loss of fine geometry details that can be captured by rendered images.

**3D Object Part Segmentation** Part segmentation is a challenging fine-grained 3D recognition task. Given a 3D scan or a mesh model, the task is to assign part category label (e.g. chair leg, cup handle) to each point or face.

We evaluate on **ShapeNet part data set** from [26], which contains 16,881 shapes from 16 categories, annotated with 50 parts in total. Most object categories are labeled with two to five parts. Ground truth annotations are labeled on sampled points on the shapes.

We formulate part segmentation as a per-point classification problem. Evaluation metric is mIoU on points. For each shape  $S$  of category  $C$ , to calculate the shape’s mIoU: For each part type in category  $C$ , compute IoU between groundtruth and prediction. If the union of groundtruth and prediction points is empty, then count part IoU as 1. Then we average IoUs for all part types in category  $C$  to get mIoU for that shape. To calculate mIoU for the category, we take average of mIoUs for all shapes in that category.

In this section, we compare our segmentation version PointNet (a modified version of Fig 2, *Segmentation Network*) with two traditional methods [24] and [26] that both take advantage of point-wise geometry features and

correspondences between shapes, as well as our own 3D CNN baseline. See supplementary for the detailed modifications and network architecture for the 3D CNN.

In Table 2, we report per-category and mean IoU(%) scores. We observe a 2.3% mean IoU improvement and our net beats the baseline methods in most categories.

We also perform experiments on simulated Kinect scans to test the robustness of these methods. For every CAD model in the ShapeNet part data set, we use Blensor Kinect Simulator [7] to generate incomplete point clouds from six random viewpoints. We train our PointNet on the complete shapes and partial scans with the same network architecture and training setting. Results show that we lose only 5.3% mean IoU. In Fig 3, we present qualitative results on both complete and partial data. One can see that though partial data is fairly challenging, our predictions are reasonable.

**Semantic Segmentation in Scenes** Our network on part segmentation can be easily extended to semantic scene segmentation, where point labels become semantic object classes instead of object part labels.

We experiment on the **Stanford 3D semantic parsing data set** [1]. The dataset contains 3D scans from Matterport scanners in 6 areas including 271 rooms. Each point in the scan is annotated with one of the semantic labels from 13 categories (chair, table, floor, wall etc. plus clutter).

To prepare training data, we firstly split points by room, and then sample rooms into blocks with area 1m by 1m. We train our segmentation version of PointNet to predict

	mean IoU	overall accuracy
Ours baseline	20.12	53.19
Ours PointNet	<b>47.71</b>	<b>78.62</b>

Table 3. **Results on semantic segmentation in scenes.** Metric is average IoU over 13 classes (structural and furniture elements plus clutter) and classification accuracy calculated on points.

	table	chair	sofa	board	mean
# instance	455	1363	55	137	
Armeni et al. [1]	46.02	16.15	<b>6.78</b>	3.91	18.22
Ours	<b>46.67</b>	<b>33.80</b>	4.76	<b>11.72</b>	<b>24.24</b>

Table 4. **Results on 3D object detection in scenes.** Metric is average precision with threshold IoU 0.5 computed in 3D volumes.



Figure 4. **Qualitative results for semantic segmentation.** Top row is input point cloud with color. Bottom row is output semantic segmentation result (on points) displayed in the same camera viewpoint as input.

per point class in each block. Each point is represented by a 9-dim vector of XYZ, RGB and normalized location as to the room (from 0 to 1). At training time, we randomly sample 4096 points in each block on-the-fly. At test time, we test on all the points. We follow the same protocol as [1] to use k-fold strategy for train and test.

We compare our method with a baseline using hand-crafted point features. The baseline extracts the same 9-dim local features and three additional ones: local point density, local curvature and normal. We use standard MLP as the classifier. Results are shown in Table 3, where our PointNet method significantly outperforms the baseline method. In Fig 4, we show qualitative segmentation results. Our network is able to output smooth predictions and is robust to missing points and occlusions.

Based on the semantic segmentation output from our network, we further build a 3D object detection system using connected component for object proposal (see supplementary for details). We compare with previous state-of-the-art method in Table 4. The previous method is based on a sliding shape method (with CRF post processing) with SVMs trained on local geometric features and global room context feature in voxel grids. Our method outperforms it by a large margin on the furniture categories reported.

## 5.2. Architecture Design Analysis

In this section we validate our design choices by control experiments. We also show the effects of our network’s hyperparameters.

### Comparison with Alternative Order-invariant Methods

As mentioned in Sec 4.2, there are at least three options for consuming unordered set inputs. We use the ModelNet40 shape classification problem as a test bed for comparisons of those options, the following two control experiment will also use this task.

The baselines (illustrated in Fig 5) we compared with include multi-layer perceptron on unsorted and sorted

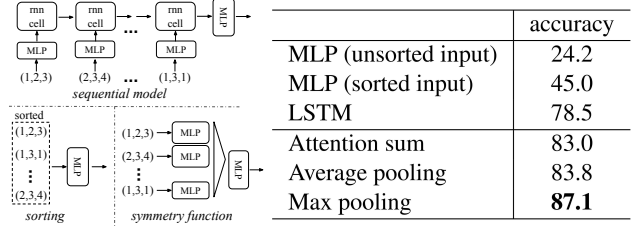


Figure 5. **Three approaches to achieve order invariance.** Multi-layer perceptron (MLP) applied on points consists of 5 hidden layers with neuron sizes 64,64,64,128,1024, all points share a single copy of MLP. The MLP close to the output consists of two layers with sizes 512,256.

points as  $n \times 3$  arrays, RNN model that considers input point as a sequence, and a model based on symmetry functions. The symmetry operation we experimented include max pooling, average pooling and an attention based weighted sum. The attention method is similar to that in [22], where a scalar score is predicted from each point feature, then the score is normalized across points by computing a softmax. The weighted sum is then computed on the normalized scores and the point features. As shown in Fig 5, max-pooling operation achieves the best performance by a large winning margin, which validates our choice.

### Effectiveness of Input and Feature Transformations

In Table 5 we demonstrate the positive effects of our input and feature transformations (for alignment). It’s interesting to see that the most basic architecture already achieves quite reasonable results. Using input transformation gives a 0.8% performance boost. The regularization loss is necessary for the higher dimension transform to work. By combining both transformations and the regularization term, we achieve the best performance.

### Robustness Test

We show our PointNet, while simple and effective, is robust to various kinds of input corruptions. We use the same architecture as in Fig 5’s max pooling network. Input points are normalized into a unit sphere. Results are in Fig 6.

As to missing points, when there are 50% points missing, the accuracy only drops by 2.4% and 3.8% w.r.t. furthest and random input sampling. Our net is also robust to outlier

Transform	accuracy
none	87.1
input (3x3)	87.9
feature (64x64)	86.9
feature (64x64) + reg.	87.4
both	<b>89.2</b>

Table 5. **Effects of input feature transforms.** Metric is overall classification accuracy on ModelNet40 test set.

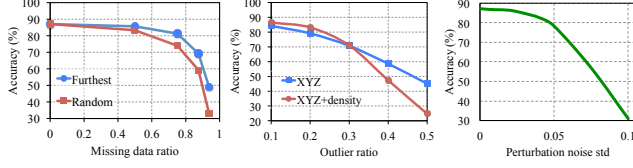


Figure 6. **PointNet robustness test.** The metric is overall classification accuracy on ModelNet40 test set. Left: Delete points. Furthest means the original 1024 points are sampled with furthest sampling. Middle: Insertion. Outliers uniformly scattered in the unit sphere. Right: Perturbation. Add Gaussian noise to each point independently.

points, if it has seen those during training. We evaluate two models: one trained on points with  $(x, y, z)$  coordinates; the other on  $(x, y, z)$  plus point density. The net has more than 80% accuracy even when 20% of the points are outliers. Fig 6 right shows the net is robust to point perturbations.

### 5.3. Visualizing PointNet

In Fig 7, we visualize some results of the **critical point sets**  $C_S$  and the **upper-bound shapes**  $N_S$  (as discussed in Thm 2) for some sample shapes  $S$ . The point sets between the two shapes will give exactly the same global shape feature  $f(S)$ .

We can see clearly from Fig 7 that the **critical point sets**  $C_S$ , those contributed to the max pooled feature, summarizes the skeleton of the shape. The **upper-bound shapes**  $N_S$  illustrates the largest possible point cloud that give the same global shape feature  $f(S)$  as the input point cloud  $S$ .  $C_S$  and  $N_S$  reflect the robustness of PointNet, meaning that losing some non-critical points does not change the global shape signature  $f(S)$  at all.

The  $N_S$  is constructed by forwarding all the points in a edge-length-2 cube through the network and select points  $p$  whose point function values  $(h_1(p), h_2(p), \dots, h_K(p))$  are

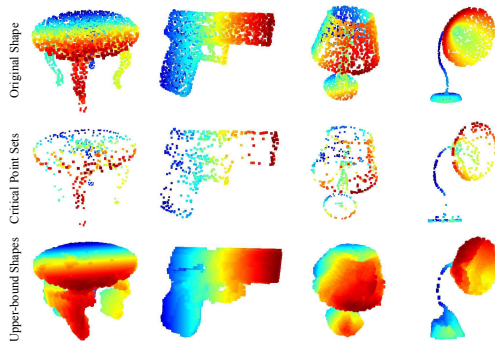


Figure 7. **Critical points and upper bound shape.** While critical points jointly determine the global shape feature for a given shape, any point cloud that falls between the critical points set and the upper bound shape gives exactly the same feature. We color-code all figures to show the depth information.

no larger than the global shape descriptor.

### 5.4. Time and Space Complexity Analysis

Table 6 summarizes space (number of parameters in the network) and time (floating-point operations/sample) complexity of our classification PointNet. We also compare PointNet to a representative set of volumetric and multi-view based architectures in previous works.

While MVCNN [20] and Subvolume (3D CNN) [16] achieve high performance, PointNet is orders more efficient in computational cost (measured in FLOPs/sample:  $141x$  and  $8x$  more efficient, respectively). Besides, PointNet is much more space efficient than MVCNN in terms of #param in the network ( $17x$  less parameters). Moreover, PointNet is much more scalable – it’s space and time complexity is  $O(N)$  – linear in the number of input points. However, since convolution dominates computing time, multi-view method’s time complexity grows *squarely* on image resolution and volumetric convolution based method grows *cubically* with the volume size.

Empirically, PointNet is able to process more than one million points per second for point cloud classification (around 1K objects/second) or semantic segmentation (around 2 rooms/second) with a 1080X GPU on TensorFlow, showing great potential for real-time applications.

	#params	FLOPs/sample
PointNet (vanilla)	0.8M	148M
PointNet	3.5M	440M
Subvolume [16]	16.6M	3633M
MVCNN [20]	60.0M	62057M

Table 6. Time and space complexity of deep architectures for 3D data classification. PointNet (vanilla) is the classification PointNet without input and feature transformations. FLOP stands for floating-point operation. The “M” stands for million. Subvolume and MVCNN used pooling on input data from multiple rotations or views, without which they have much inferior performance.

## 6. Conclusion

In this work, we propose a novel deep neural network *PointNet* that directly consumes point cloud. Our network provides a unified approach to a number of 3D recognition tasks including object classification, part segmentation and semantic segmentation, while obtaining on par or better results than state of the arts on standard benchmarks. We also provide theoretical analysis and visualizations towards understanding of our network.

**Acknowledgement.** The authors gratefully acknowledge the support of a Samsung GRO grant, ONR MURI N00014-13-1-0341 grant, NSF grant IIS-1528025, a Google Focused Research Award, a gift from the Adobe corporation and hardware donations by NVIDIA.



## References

- [1] I. Armeni, O. Sener, A. R. Zamir, H. Jiang, I. Brilakis, M. Fischer, and S. Savarese. 3d semantic parsing of large-scale indoor spaces. In *Proceedings of the IEEE International Conference on Computer Vision and Pattern Recognition*, 2016. 6, 7
- [2] M. Aubry, U. Schlickewei, and D. Cremers. The wave kernel signature: A quantum mechanical approach to shape analysis. In *Computer Vision Workshops (ICCV Workshops), 2011 IEEE International Conference on*, pages 1626–1633. IEEE, 2011. 2
- [3] M. M. Bronstein and I. Kokkinos. Scale-invariant heat kernel signatures for non-rigid shape recognition. In *Computer Vision and Pattern Recognition (CVPR), 2010 IEEE Conference on*, pages 1704–1711. IEEE, 2010. 2
- [4] J. Bruna, W. Zaremba, A. Szlam, and Y. LeCun. Spectral networks and locally connected networks on graphs. *arXiv preprint arXiv:1312.6203*, 2013. 2
- [5] D.-Y. Chen, X.-P. Tian, Y.-T. Shen, and M. Ouhyoung. On visual similarity based 3d model retrieval. In *Computer graphics forum*, volume 22, pages 223–232. Wiley Online Library, 2003. 2
- [6] Y. Fang, J. Xie, G. Dai, M. Wang, F. Zhu, T. Xu, and E. Wong. 3d deep shape descriptor. In *Proceedings of the IEEE Conference on Computer Vision and Pattern Recognition*, pages 2319–2328, 2015. 2
- [7] M. Gschwandtner, R. Kwitt, A. Uhl, and W. Pree. BlenSor: Blender Sensor Simulation Toolbox Advances in Visual Computing. volume 6939 of *Lecture Notes in Computer Science*, chapter 20, pages 199–208. Springer Berlin / Heidelberg, Berlin, Heidelberg, 2011. 6
- [8] K. Guo, D. Zou, and X. Chen. 3d mesh labeling via deep convolutional neural networks. *ACM Transactions on Graphics (TOG)*, 35(1):3, 2015. 2
- [9] M. Jaderberg, K. Simonyan, A. Zisserman, et al. Spatial transformer networks. In *NIPS 2015*. 4
- [10] A. E. Johnson and M. Hebert. Using spin images for efficient object recognition in cluttered 3d scenes. *IEEE Transactions on pattern analysis and machine intelligence*, 21(5):433–449, 1999. 2
- [11] M. Kazhdan, T. Funkhouser, and S. Rusinkiewicz. Rotation invariant spherical harmonic representation of 3 d shape descriptors. In *Symposium on geometry processing*, volume 6, pages 156–164, 2003. 5
- [12] Y. Li, S. Pirk, H. Su, C. R. Qi, and L. J. Guibas. Fpnn: Field probing neural networks for 3d data. *arXiv preprint arXiv:1605.06240*, 2016. 2
- [13] H. Ling and D. W. Jacobs. Shape classification using the inner-distance. *IEEE transactions on pattern analysis and machine intelligence*, 29(2):286–299, 2007. 2
- [14] J. Masci, D. Boscaini, M. Bronstein, and P. Vandergheynst. Geodesic convolutional neural networks on riemannian manifolds. In *Proceedings of the IEEE International Conference on Computer Vision Workshops*, pages 37–45, 2015. 2
- [15] D. Maturana and S. Scherer. Voxnet: A 3d convolutional neural network for real-time object recognition. In *IEEE/RSJ International Conference on Intelligent Robots and Systems*, September 2015. 2, 5
- [16] C. R. Qi, H. Su, M. Nießner, A. Dai, M. Yan, and L. Guibas. Volumetric and multi-view cnns for object classification on 3d data. In *Proc. Computer Vision and Pattern Recognition (CVPR), IEEE*, 2016. 2, 5, 8
- [17] R. B. Rusu, N. Blodow, and M. Beetz. Fast point feature histograms (fpfh) for 3d registration. In *Robotics and Automation, 2009. ICRA'09. IEEE International Conference on*, pages 3212–3217. IEEE, 2009. 2
- [18] R. B. Rusu, N. Blodow, Z. C. Marton, and M. Beetz. Aligning point cloud views using persistent feature histograms. In *2008 IEEE/RSJ International Conference on Intelligent Robots and Systems*, pages 3384–3391. IEEE, 2008. 2
- [19] M. Savva, F. Yu, H. Su, M. Aono, B. Chen, D. Cohen-Or, W. Deng, H. Su, S. Bai, X. Bai, et al. Shrec16 track large-scale 3d shape retrieval from shapenet core55. 2
- [20] H. Su, S. Maji, E. Kalogerakis, and E. G. Learned-Miller. Multi-view convolutional neural networks for 3d shape recognition. In *Proc. ICCV, to appear*, 2015. 2, 5, 6, 8
- [21] J. Sun, M. Ovsjanikov, and L. Guibas. A concise and provably informative multi-scale signature based on heat diffusion. In *Computer graphics forum*, volume 28, pages 1383–1392. Wiley Online Library, 2009. 2
- [22] O. Vinyals, S. Bengio, and M. Kudlur. Order matters: Sequence to sequence for sets. *arXiv preprint arXiv:1511.06391*, 2015. 2, 4, 7
- [23] D. Z. Wang and I. Posner. Voting for voting in online point cloud object detection. *Proceedings of the Robotics: Science and Systems, Rome, Italy*, 1317, 2015. 2
- [24] Z. Wu, R. Shou, Y. Wang, and X. Liu. Interactive shape co-segmentation via label propagation. *Computers Graphics*, 38:248 – 254, 2014. 6
- [25] Z. Wu, S. Song, A. Khosla, F. Yu, L. Zhang, X. Tang, and J. Xiao. 3d shapenets: A deep representation for volumetric shapes. In *Proceedings of the IEEE Conference on Computer Vision and Pattern Recognition*, pages 1912–1920, 2015. 2, 5
- [26] L. Yi, V. G. Kim, D. Ceylan, I.-C. Shen, M. Yan, H. Su, C. Lu, Q. Huang, A. Sheffer, and L. Guibas. A scalable active framework for region annotation in 3d shape collections. *SIGGRAPH Asia*, 2016. 6